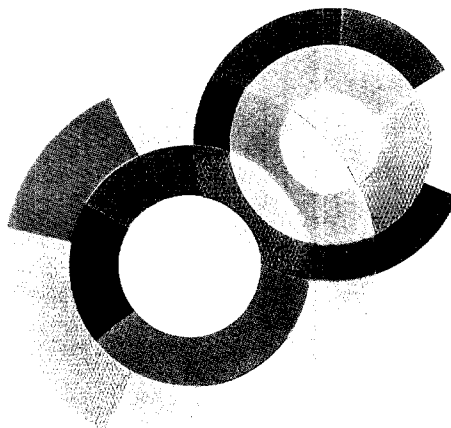
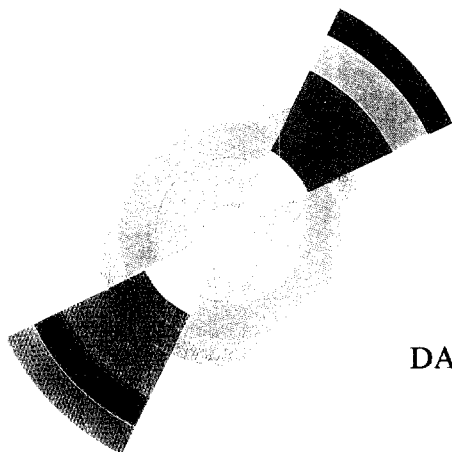
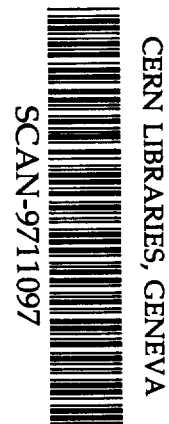
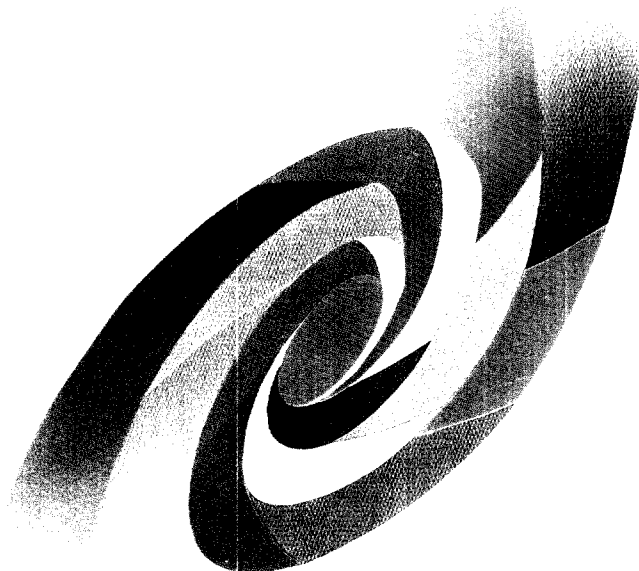


AC

cea
C.E. SACLAY
DSM

SERVICE DE PHYSIQUE DES PARTICULES



DAPNIA/SPP 97-25

October 1997

**DIS AND DIFFRACTIVE STRUCTURE FUNCTIONS IN
THE QCD DIPOLE MODEL**

C. Royon

*Invited Talk given at the Madrid Workshop on low x Physics,
Miraflores de la Sierra (Spain), June 18-21 1997*

DAPNIA

Le DAPNIA (Département d'Astrophysique, de physique des Particules, de physique Nucléaire et de l'Instrumentation Associée) regroupe les activités du Service d'Astrophysique (SAp), du Département de Physique des Particules Élémentaires (DPhPE) et du Département de Physique Nucléaire (DPhN).

Adresse : DAPNIA, Bâtiment 141
CEA Saclay
F - 91191 Gif-sur-Yvette Cedex

DIS AND DIFFRACTIVE STRUCTURE FUNCTIONS IN THE QCD DIPOLE MODEL ^a

C. Royon

*CEA, DAPNIA, Service de Physique des Particules,
Centre d'Etudes de Saclay, France*

The proton structure function F_2 , the gluon density F_G , and the longitudinal structure function F_L are derived in the QCD dipole picture of BFKL dynamics. We use a four parameter fit to describe the 1994 H1 proton structure function F_2 data in the low x , moderate Q^2 range. Without any additional parameter, the gluon density and the longitudinal structure functions are predicted. The diffractive dissociation processes are also discussed within the same framework, and a new prediction for the proton diffractive structure function is obtained.

1 Introduction

Considering the phenomenological discussion on the proton structure functions measured by deep-inelastic scattering of electrons and positrons at HERA, it is striking to realize that the proposed models, on one side for the total quark structure function ¹ $F_2(x, Q^2)$ and on the other side for its diffractive component ² $F_2^{D(3)}(x, M^2, Q^2)$ are in general distinct. Indeed, most models ³ aiming at the description of $F_2(x, Q^2)$ use a QCD-inspired “hard Pomeron” parametrisation related either to a DGLAP ⁴ evolution with extrapolation at small- x ⁵ or to BFKL ⁶ dynamics. On the other hand, the models proposed for the diffractive component of the quark structure function are, for most of them, relying on a “soft Pomeron” picture of diffraction, assuming a point-like structure of the Pomeron considered as a compound particle ⁷.

However, the quest for an unifying picture of total and diffractive structure functions based on a perturbative QCD framework is a challenge. The interest of using the QCD dipole approach ⁸ for deep-inelastic structure functions is to deal with an unified approach based on the BFKL resummation properties of perturbative QCD. Indeed, starting from an unique non-perturbative input in terms of a primordial proton distribution of dipoles at low scale Q_0 , it is possible to compute the theoretical predictions ¹⁰ for the (transverse and longitudinal) quark and the gluon distributions as functions of x and Q^2 . In the same framework it is also possible to compute the two components of the dipole-model predictions for hard diffractive structure functions, namely the

^aInvited talk given at the Madrid low x workshop, Miraflores de la Sierra, June 18-21 1997

inelastic component ¹¹ (hereafter named component I) and the quasi-elastic one ¹² (hereafter component II), as recalled later on.

2 BFKL dynamics in the framework of the QCD dipole model

To obtain the proton structure function F_2 , we use the k_T factorisation theorem ⁹, valid at high energy (small x), to factorise the $(\gamma g(k) \rightarrow q \bar{q})$ cross section and the unintegrated gluon distribution of an onium state which contains the physics of the BFKL pomeron ⁸. One can show that ¹⁰:

$$F_2^{proton}(x, Q^2; Q_0^2) = \frac{2\bar{\alpha}N_c}{\pi} \int \frac{d\gamma}{2i\pi} h(\gamma) \frac{v(\gamma)}{\gamma} w(\gamma) \left(\frac{Q^2}{Q_0^2}\right)^\gamma e^{\frac{\bar{\alpha}N_c}{\pi} \chi(\gamma) \ln(\frac{c}{x})}$$

where h , ω , Q_0^2 and c are respectively the $(\gamma g(k) \rightarrow q \bar{q})$ cross section, the Mellin transform probability of finding an onium of transverse mass M^2 , a typically non perturbative proton scale Q_0^2 and the 'time' scale for the formation of the interacting dipoles. We can use this generic result to make predictions for F_T , F_L , and F_G knowing the $h(\gamma)$ functions. The detailed calculations can be found in ¹⁰.

The integral in γ is performed by the steepest descent method. The saddle point is at $\gamma_C = \frac{1}{2}(1 - a \ln \frac{Q}{Q_0})$ where $a = (\frac{\bar{\alpha}N_c}{\pi} 7\zeta(3) \ln \frac{c}{x})^{-1}$. It can be shown that this approximation is valid when $\ln Q/Q_0 / \ln(1/x) \ll 1$, that is in the kinematic domain of small x , and moderate Q/Q_0 . We obtain:

$$F_2 \equiv F_T + F_L = \mathcal{N} a^{1/2} e^{(\alpha_P - 1) \ln \frac{1}{x}} \frac{Q}{Q_0} e^{-\frac{\alpha}{2} \ln^2 \frac{Q}{Q_0}} \quad (1)$$

where $\alpha_P - 1 = \frac{4\bar{\alpha}N_c \ln 2}{\pi}$. The free parameters for the fit of the H1 data are \mathcal{N} , α_P , Q_0 , and c . It is possible to compare the results with the values of α_P predicted by theory. Finally, we get R , and F_G/F_2 , which are independent of the overall normalisation \mathcal{N} :

$$\begin{aligned} \frac{F_G}{F_2} &= \frac{1}{h_T + h_L} \Big|_{\gamma=\gamma_C} \\ &\equiv \frac{3\pi\gamma_C}{\bar{\alpha}} \frac{1 - \frac{2}{3}\gamma_C}{1 + \frac{3}{2}\gamma_C - \frac{3}{2}\gamma_C^2} \frac{\Gamma(2-2\gamma_C)\Gamma(2+2\gamma_C)}{(\Gamma(1-\gamma_C)\Gamma(1+\gamma_C))^3} \end{aligned} \quad (2)$$

$$R = \frac{h_L}{h_T}(\gamma_C) = \frac{\gamma_C(1-\gamma_C)}{(1+\gamma_C)(1-\frac{\gamma_C}{2})} \quad (3)$$

where γ_C is the saddle point value (see above).

3 F_2 fit and prediction for F_G and R

In order to test the accuracy of the F_2 parametrisation obtained in formula (1), a fit using the recently published data from the H1 experiment¹ has been performed¹⁰. We have only used the points with $Q^2 \leq 150 \text{GeV}^2$ to remain in a reasonable domain of validity of the QCD dipole model. The result of the fit is given in Figure 1. The χ^2 is 88.7 for 130 points, and the values of the parameters are $Q_0 = 0.522 \text{GeV}$, $\mathcal{N} = 0.059$, and $c = 1.750$, while $\Delta_P = 0.282$. Commenting on the parameters, let us note that the effective coupling constant extracted using (3) from Δ_P is $\alpha = 0.11$, close to $\alpha(M_Z)$ used in the H1 QCD fit. It is an acceptable value for the small fixed value of the coupling constant required by the BFKL framework. The running of the coupling constant is not taken into account in the present BFKL scheme. Only when next leading log calculations will be available, this will be possibly taken into account. This could explain the rather low value of the effective Δ_P which is expected to be decreased by the next leading corrections. The value of Q_0 corresponds to a transverse size of 0.4 fm which is in the correct range for a proton non-perturbative characteristic scale. The value of \mathcal{N} determines the amount of primordial dipoles in the proton to be

$$\omega(1/2) = \mathcal{N} \frac{128}{11\pi \alpha^2 N_c e_f^2} \sqrt{\frac{\pi}{2}} \simeq 7.55/e_f^2,$$

The parameter c sets the “time” scale for the formation of the interacting dipoles. It defines the effective total rapidity interval which is $\log(1/x) + \log c$, the constant being not predictable (but of order 1) at the leading logarithmic approximation.

4 Diffractive structure functions

The success of the dipole model applied to the proton structure function motivates its extension to the investigations to other inclusive processes, in particular to diffractive dissociation. We can distinguish two different components: - the “elastic” term which represents the elastic scattering of the onium on the target proton; - the “triple-pomeron” term which represents the sum of all dipole-dipole interactions (it is dominant at large masses of the excited system).

Let us describe in more details each of the two components. The “triple-pomeron” term dominates at low β , where $\beta = x/x_P$, x_P is the proton momentum fraction carried by the “pomeron”¹¹. This component, integrated over t , the momentum transfer, is factorisable in a part depending only on x_p

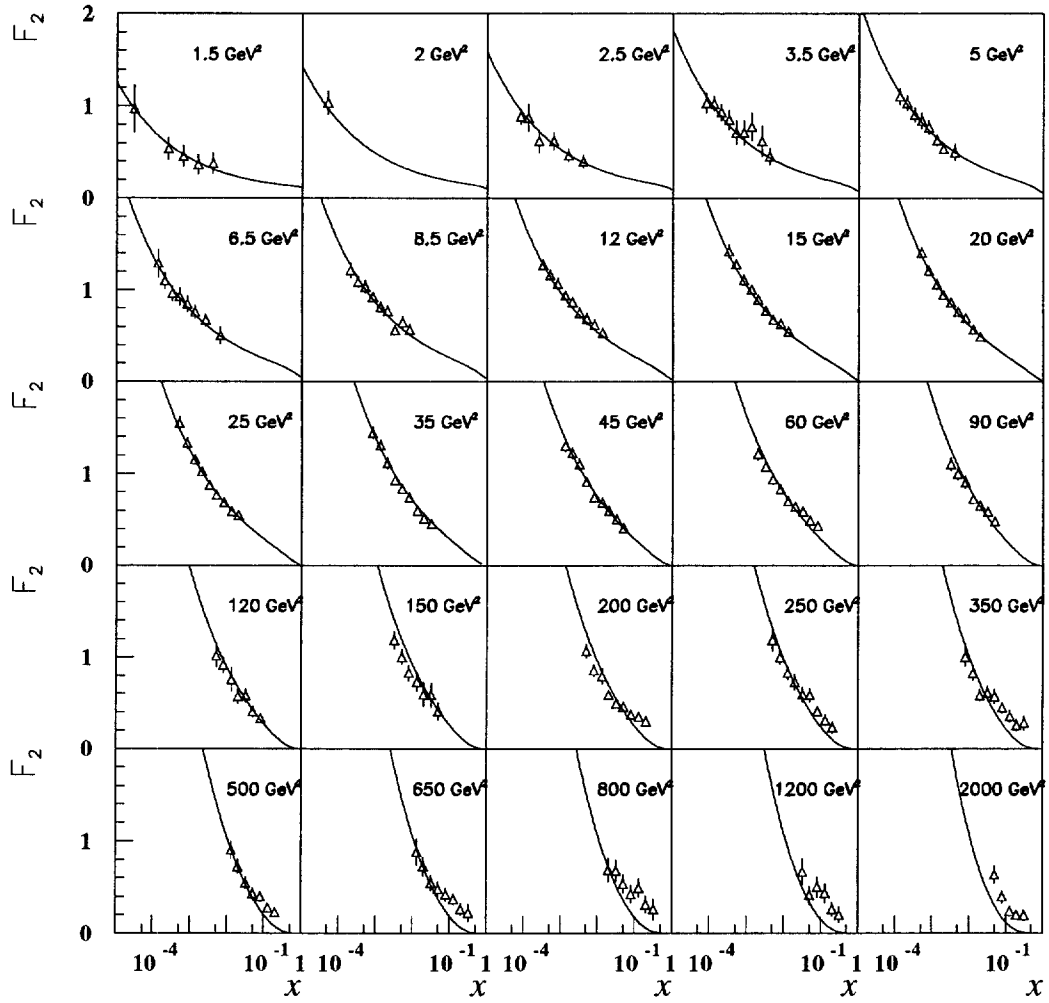


Figure 1: Results of the 3-parameter fit of the H1 proton structure function (the fit has been performed using the points with $Q^2 \leq 150 \text{ GeV}^2$)

(flux factor) and on a part depending only on β and Q^2 ("pomeron" structure function)¹¹.

$$F_2^{D(3)}(Q^2, x_p, \beta) = \Phi(x_p) F_P(Q^2, \beta) \quad (4)$$

$$\Phi(x_p) = x_p^{1-2\alpha_P} \left(\frac{2a(x_p)}{\pi} \right)^3 \quad (5)$$

where a is defined in the first chapter, which gives the following formula for the inelastic component:

$$F_2^{D(3),I} \simeq x_p^{-1-2\Delta_P} \left(\frac{2a}{\pi} \right)^3 \left(\frac{Q}{Q_0} \right) (\beta)^{-\Delta_P} \left(\frac{2a(\beta)}{\pi} \right)^{1/2} \exp \left\{ -\frac{1}{2} a(\beta) \ln^2 \left(\frac{Q}{Q_0} \right) \right\} \quad (6)$$

The important point to notice is that $a(x_p)$ is proportional of $\ln 1/x_p$. The effective exponent (the slope of $\ln F_2^D$ in $\ln x_p$) is found to be dependant on x_p because of the term in $\ln^3(x_p)$ coming from a , and is sizeably smaller than the BFKL exponent. This is why we can describe an apparently soft behaviour (a small exponent in x_p) with the BFKL equation, which predicts a hard behaviour (the exponent in x_p is close to 0.35). This is due to the fact that the effective exponent is smaller then the real one. It should be also noticed that the structure function F is directly proportional to the proton structure function.

For the elastic component, one considers

$$F_T^{D(3),II} \simeq \left(\frac{x_P}{c} \right)^{-2\Delta_P} a \left(\frac{x_P}{c} \right)^3 \left(\frac{Q}{Q_0} \right)^2 \times \\ \times \int_{\frac{2\lambda}{Q_0}}^{\infty} 2b db \int_0^1 dz z^2 (1-z^2) (z^2 + (1-z)^2) \times \\ \left| \int_0^{\min(b, \frac{2}{Q_0})} \frac{X^2 dX}{b^2} \log \left(\frac{8Q_0 b^2}{X} \right) e^{-\frac{\alpha(x_P)}{2} \log^2 \left(\frac{8Q_0 b^2}{X} \right)} K_1(\hat{Q}X) J_1(\hat{M}X) \right|^2 \quad (7)$$

and adds $F_L^{D(3)II}$ where F_L is obtained from (36) by changing $\{z^2 + (1-z)^2\}$ into $\{4z(1-z)\}$ and $[K_1(\hat{Q}X) J_1(\hat{M}X)]$ by $[K_0(\hat{Q}X) J_0(\hat{M}X)]$. The elastic component behaves quite differently¹². First it dominates at $\beta \sim 1$. It is also factorisable like the inelastic component, but with a different flux factor, which means that the sum of the two components will not be factorisable.

This means that in this model, factorisation breaking is coming from the fact that we sum up two factorisable components with different flux factors. The β dependence is quite flat at large β , due to the interplay between the longitudinal and transverse components. The sum remains almost independent of β , whereas the ratio $R = F_L/F_T$ is strongly β dependent. Once more, a R measurement in diffractive processes will be an interesting way to distinguish the different models, as the dipole model predicts different β and Q^2 behaviours.

The sum of the two components shown in figure 2 describes quite well the H1 data. There is no further fit of the data as we chose to take the different parameters (Q_0, α_P, c) from the F_2 fit. In this study, the normalisation is left free. The most striking point is that we describe quite well the factorisation breaking due to the resummation of the two components at low and large β ¹³. The full line is the sum of the two components, the dashed line the inelastic one (which dominates at low β), and the dotted line the elastic one (which dominates at high β).

Acknowledgments

The results described in the present contribution come from a fruitful collaboration with A.Bialas, H.Navelet, and R.Peschanski. I also thank R.Peschanski for reading and comments on the manuscript.

References

1. H1 coll., *Nucl.Phys. B* **470** (1996) 3
2. H1 coll., "Inclusive measurement of Diffractive Deep-Inelastic Scattering", DESY 97-158, August 1997.
3. For a recent review, see J.Blumlein, J.Huston, C.Royon, R.Yoshida, *Summary of Working group I: hadron structure*, P.Newman, *Colour singlet exchange in ep interactions*, D.Soper, *Diffraction in DIS and elsewhere*, Summary talks given at the DIS97 conference, Chicago
4. G. Altarelli and G. Parisi, *Nucl. Phys.* **B126** (1977) 298; V.N. Gribov and L.N. Lipatov, *Sov. Journ. Nucl. Phys.* **15** (1972) 438 and 675.
5. M.Glück, E.Reya, A.Vogt, *Z.Phys.* **C53** (1992) 127, *Phys.Lett.* **B306** (1993) 391
6. V.S.Fadin, E.A.Kuraev, L.N.Lipatov *Phys. Lett.* **B60** (1975) 50; I.I.Balitsky and L.N.Lipatov, *Sov.J.Nucl.Phys.* **28** (1978) 822.
7. G.Ingelman, P.Schlein, *Phys.Lett.* **B152** (1985) 256
8. A.H.Mueller and B.Patel, *Nucl. Phys.* **B425** (1994) 471., A.H.Mueller, *Nucl. Phys.* **B437** (1995) 107., A.H.Mueller, *Nucl. Phys.* **B415**

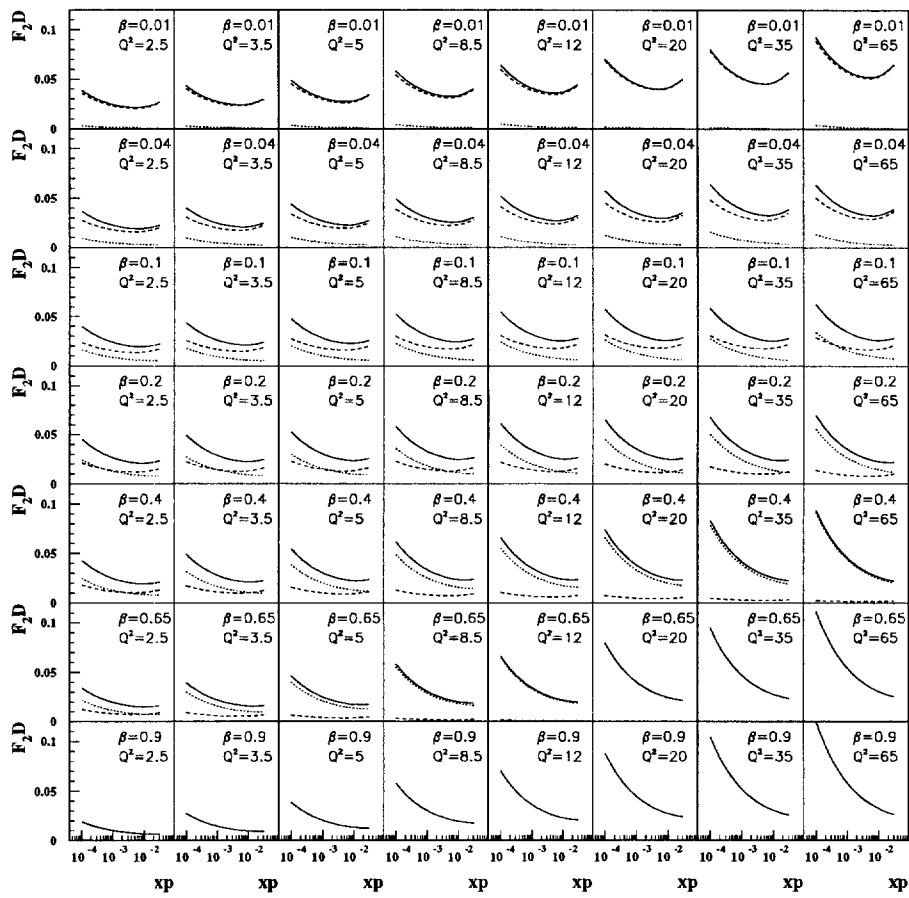


Figure 2: Prediction on F2D (cf text)

- (1994) 373; See also, in a somewhat r elated approach: N.N.Nikolaev and B.G.Zakharov, *Zeit. für. Phys.* **C49** (1991) 607.
9. S.Catani, M.Ciafaloni and Hautmann, *Phys. Lett.* **B242** (1990) 97; *Nucl. Phys.* **B366** (1991) 135; J.C.Collins and R.K.Ellis, *Nucl. Phys.* **B360** (1991) 3; S.Catani and Hautmann, *Phys. Lett.* **B315** (1993) 157; *Nucl. Phys.* **B427** (1994) 475
 10. H.Navelet, R.Peschanski, Ch.Royon, and S.Wallon, *Phys.Lett.*, **B385**, (1996) 357, H.Navelet, R.Peschanski, Ch.Royon, *Phys.Lett.*, **B366**, (1996) 329.
 11. A.Bialas, R.Peschanski, *Phys. Lett.* **B378** (1996) 302, A.Bialas, *Acta Phys.Pol.* **B27** (1996) no. 6
 12. A.Bialas, R.Peschanski, *Phys.Lett.* *B387* (1996) 405
 13. A.Bialas, R.Peschanski, C.Royon, to appear